Hindawi
Scientific Programming
Volume 2021, Article ID 6872291, 11 pages
https://doi.org/10.1155/2021/6872291

Research Article

Dual X-Ray Image under Neural Network Adopted in Comparison of Efficacy and Safety of Deep Hydrolyzed Protein Milk Powder and Parenteral Nutrition in Intervention of Neonatal Noninfectious Abdominal Distension

Yinghong Zong,[1] **Limei Wu**,[2] **Dongping Wu**,[1] **Jing Jiang**,[2] **and Shimei Yang**[2]

[1]*Department of Pediatrics, Yiwu Central Hospital, Yiwu 32000, Zhejiang, China*
[2]*Department of Pediatrics, Yiwu Maternity and Children Hospital, Yiwu 32000, Zhejiang, China*

Correspondence should be addressed to Shimei Yang; 2020162364@stu.cpu.edu.cn

Received 27 September 2021; Revised 8 November 2021; Accepted 10 November 2021; Published 16 December 2021

Academic Editor: M. Pallikonda Rajasekaran

Objective. The aim of this study was to explore the application value of double X-ray image based on neural network in comparison of the efficacy and safety of deep-water proteolytic milk powder and parenteral nutrition in the intervention of neonatal noninfectious abdominal distention. *Methods*. Clinical data of 58 neonates diagnosed with noninfectious abdominal distention were retrospectively analyzed. 2D-3D registration was simplified into two steps by decomposing spatial rigid-body transformation parameters into two planes, including 2D-2D approximate rigid-body registration and single-parameter 2D-3D rigid-body registration. Then, the convolution neural network was used to fit the nonlinear mapping relationship between the residual of X-ray images and the corresponding attitude differences of children, and the residual regression spatial rigid-body transformation parameters of the X-DRR image pairs were obtained. Noninfectious abdominal distention was diagnosed in all neonates, of which 28 neonates were treated with deep hydrolyzed protein milk powder. Another 30 neonates who received parenteral nutrition support were set as control group. All newborns received two weeks of treatment. The total effective rate, birth weight recovery, weight growth rate, intestinal feeding recovery time, and incidence of feeding intolerance were compared between the two groups. *Results*. Spatial coordinate decomposition using double X-ray can simplify the mapping relationship between spatial coordinate transformation and X-DRR residual image. Compared with the gray level iterative optimization registration algorithm, the registration accuracy and speed were significantly improved. The total effective rate in the treatment group (92.86%) was significantly higher than that in the control group (9%). The recovery time of birth weight, intestinal feeding recovery time, and meconium excretion time were significantly shorter than those in the control group, and the body weight in the treatment group increased faster than that in the control group ($P < 0.05$). In addition, the incidence of feeding intolerance was 3.57% (1/28) in the treatment group and 36.36% (8/22) in the control group, which was significantly lower than that in the treatment group ($P < 0.05$). *Conclusion*. After data training, the network can complete accurate double ray registration in 0.04 s. Deep hydrolyzed protein milk powder had remarkable therapeutic effect on neonates, with no infective abdominal distention, fast recovery, and low incidence of feeding intolerance, which was safe and reliable in clinical application.

1. Introduction

Abdominal distention is a common disease of newborns. It is often a complication of multiple diseases of newborns, which affects their breathing and heart rate, and often accompanies other serious diseases. Therefore, it is necessary to diagnose the causes in time and make treatment as early as possible [1, 2]. Neonatal abdominal distention is generally divided into infectious and noninfectious. Infectious abdominal distention is caused by a variety of viruses and bacteria. The disease develops rapidly, often with serious water electrolyte disorder and other critical symptoms [3]. Noninfectious

abdominal distention is mild, usually caused by stress reactions caused by other serious diseases or by the inhalation of a large amount of air by the newborn. Although the symptoms of noninfective abdominal distention are not serious, children often have dyspepsia and other symptoms, so they also need to be treated carefully [4].

The traditional intelligent image diagnosis method was to compare the automatically marked or segmented area with the predefined reference template, but it still needed the final diagnosis result from the imaging expert. In the application of disease diagnosis, double X-ray imaging was the most important imaging method in the clinical diagnosis and follow-up of noninfectious abdominal distension, which was widely used in lesion detection, segmentation, and diagnosis. Because different lesion types correspond to different characteristics, how to separate lesion areas from images was the key to the success of high-precision diagnosis system. With the application of artificial intelligence in computers, deep learning has been widely used in organ segmentation and lesion detection tasks in CT images [5, 6]. Deep learning methods include target detection network, image segmentation network, and classification network [7, 8]. CT organ image segmentation method based on deep learning and CT lesion image segmentation method based on deep learning algorithm, as well as lesion target detection method based on deep learning algorithm, have significantly improved the diagnostic efficiency of diseases in the application [9]. In current medical technology, the use of image-guided radiotherapy can also reduce side effects while ensuring the accuracy of radiotherapy. The 2D-3D medical image registration technology can calculate the positioning error. The traditional 2D-3D registration algorithm usually uses the way of wearing a butterfly, which uses the spatial posture of CT to generate digitally reconstructed radiographic images (DRR). The similarity of the X-ray images acquired in the image determines the difference between the CT posture and the patient's posture. Lei and Yan [10] used the combination of coarse registration of two single panels on a pair of orthogonal X-ray images as 2D3D registration initialization to reduce the number of iterations. Ghafurian et al. [11] used a new image gradient probability density histogram as an image feature to optimize the transformation vector of degrees of freedom. With the continuous and in-depth application of deep learning in medical imaging, some scholars also applied convolutional neural networks to image residuals to change the parameters of the rigid body transformation in CT space.

Deep hydrolyzed protein milk powder was to hydrolyze milk protein with enzyme, and after heating and ultrafiltration, more than 95% of milk protein was short peptide with molecular weight less than 3000 daltons. Compared with whole protein, short peptide and amino acid were easier to digest and absorb, which was more suitable for children with immature digestive tract and low digestive enzyme activity. Some studies had found that deep hydrolyzed protein could promote gastric emptying of premature infants, promote gastrointestinal hormone secretion, and shorten the transit time of milk in gastrointestinal tract, thus reducing the incidence of gastroesophageal reflux and feeding intolerance in premature infants and achieving total intestinal nutrition as soon as possible and so shortening the time of parenteral nutrition and reducing the complications of parenteral nutrition.

Through measurement, assessment, classification, diagnosis, and preoperative design, deep learning-based images can assist physicians to make early disease diagnosis, positive treatment plans, and effective clinical decisions. It can effectively improve the efficiency of medical imaging in disease detection, recognition, and diagnosis and then promote and realize computer-assisted therapy in the medical and health field [12]. In this study, an iteratively optimized medical image registration algorithm was proposed to improve the registration speed of medical images by applying deep hydrolyzed protein milk powder and parenteral nutrition in the treatment of neonatal noninfectious abdominal distension. 2D-3D registration was simplified into two steps, including 2D-2D approximate rigid body registration and single-parameter 2D-3D rigid body registration. Then, the convolution neural network was used to fit the nonlinear mapping relationship between the residual of the X-ray images of children and their corresponding attitude differences. The residual regression spatial rigid-body transformation parameters of the X-DRR images were obtained, and fast 2D-3D registration was realized, thus providing reference for clinical diagnosis of abdominal distension in children.

2. General Materials and Methods

2.1. Convolutional Neural Network. Convolutional neural network (CNN) is a kind of feedforward neural network that contains convolutions and has deep learning results and is one of the representative algorithms of deep learning. Convolutional neural network has constant learning ability and can classify input information according to its level. The parameter sharing of convolutional kernel in the hidden layer and the sparsity of interlayer connections enable the convolutional neural network to learn lattice features, such as pixel and audio, with a small amount of computation, with a stable effect and no need for additional features of data. Figure 1 shows the structure of convolutional neural network.

2.2. X-Ray Geometric Decomposition. Dual X-rays establish a spatial coordinate system and decompose two plane coordinate systems. The geometric diagram is shown in Figures 2 and 3. The ray source $X1\ \overline{O}1$ and the ray source $X2\ \overline{O}2$ have an angle θ around the Y axis, and both rays are parallel to plane 0.

In the geometric relationship, the spatial parameter decomposes the X-ray image into a plane coordinate system. R rotates along the XY axis, RX, RY, scale represents the scaling factor, and the equation for decomposing the spatial parameter to the plane parameter is as follows:

$$Tx1 = \text{scale}1 \times Tx\ r1 = Rz$$

$$Tx1 = \text{scale}1 \times Ty$$

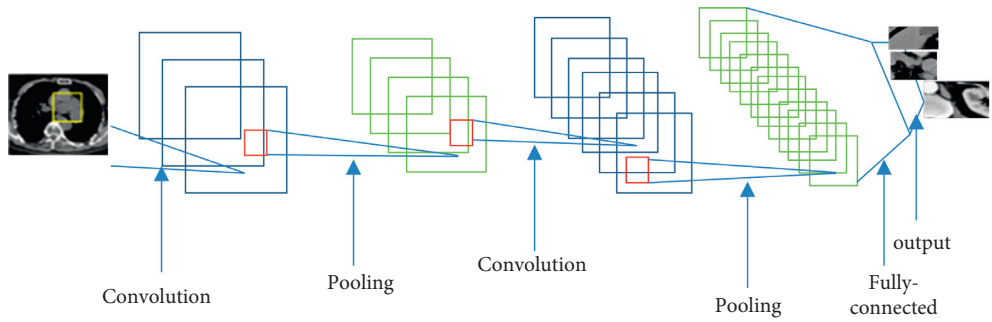

Figure 1: Schematic diagram of convolutional neural network.

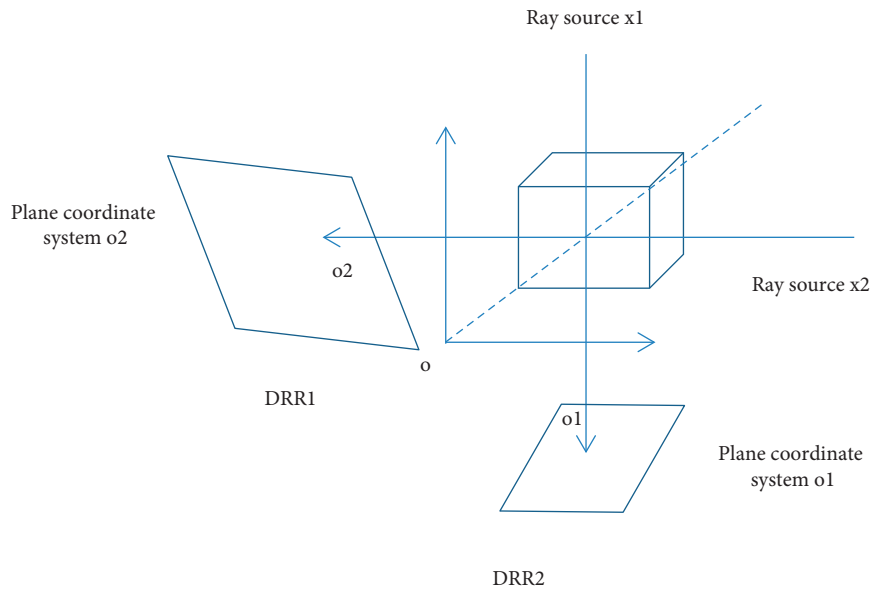

Figure 2: The geometric relationship between the space coordinate system and a pair of orthogonal plane coordinate systems.

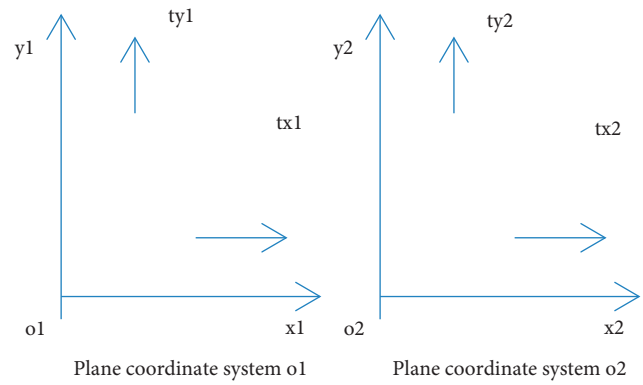

Figure 3: The geometrical schematic diagram of two orthogonal plane coordinate systems.

$$Ty2 = -\text{scale2} \times Ty \; r2 = RX \times \sin(\theta) + Rz \times \cos(\theta)$$
$$Tx2 = -\text{scale2} \times (Tx \times \cos(\theta) \; Tz \times \sin(X\theta))$$

The distance from the ray source to the digitally reconstructed radiographic image plane is the source image distance (SID), and SAD represents the distance from the ray source to the isocenter. Then, the scaling factor is calculated as follows:

Scale =

$$\begin{aligned} \text{scale1} &= \frac{\text{SID}}{\text{SAD} + TY}, \\ \text{scale2} &= \frac{\text{SID}}{\text{SAD} + (TX \times \sin\theta + Tz \times \cos\theta)}. \end{aligned} \tag{1}$$

After simulated shooting, the angled ray images are simulated in the above-mentioned coordinate system to generate two DRR plane images, and the coordinate system is decomposed to obtain accurate pairing of X-DRR images on the two planes. Then, the spatial parameters are calculated.

2.3. Step-by-Step Registration. The X-DRR image under the rays is formed in the space of the CT pose, and the transformation from the residual error in the image to the spatial pose also has a highly nonlinear mapping. The neural network wirelessly approximates any nonlinear function, and the rotation parameter appears as a rotation in the DRR image. At the same time, the light path from the ray source to the pixel of another DRR image changes through the CT pixel. The specific process of distribution regression is shown in Figure 4.

2.4. Network Structure. After the use of three convolutional neural networks (CNN), the parameters of the two planes are returned to ensure the consistency of the network framework. For the residual image of the input X-DRR image pair, a 512×512 image is divided into four 258×258 areas that overlap each other, which can reduce the size of the input image. The overlapping images are input to a feature extraction network composed of only a few convolutional layers, and then the amplified feature map is input to the feature extraction network composed of dense block. All images are obtained through the feature fusion operation of 1×1 convolutional layer after the feature dull agreement is passed through different pooling layers, and the pooling result is input to the connection layer to output the placement error of the patient. The internal structure of the network is shown in Table 1. Figure 5 shows the main framework of the network. RELU is the activation function. The conv2D-1 uses deep separable convolution, conv2D-5 uses 1×1 convolution kernel for feature fusion, and other convolution kernels are 3×3. The image processing in the third network can remove the error introduced at the edge of the image when the two residual images are around the edge of the plane, and the result of the segmented image is taken as the output image of the network.

2.5. Subjects. The clinical data of 58 neonates who were diagnosed as noninfectious abdominal distension in our hospital from July, 2017, to July, 2019, were retrospectively analyzed. The main complaint and physical examination of the parents confirmed that the child had abdominal distention, and the child was diagnosed as having noninfectious abdominal distention. Among them, 30 cases swallowed a lot of gas during crying or lactation, 12 cases were neonatal jaundice, 10 cases were neonatal malnutrition, 5 cases were neonatal hypoxic-ischemic encephalopathy, and 3 cases were neonatal intracranial hemorrhage. There were 21 premature infants and 47 full-term infants. 28 cases were fed with deeply hydrolyzed protein milk powder as the treatment group, and 30 children who received parenteral nutrition support were classified as the control group. There were 16 males and 12 females in the treatment group, with an average gestational age of 37.82 ± 2.02 weeks, an average birth weight of 2.38 ± 0.72 kg, and an average age of admission of 3.63 ± 0.23 days. There were 17 males and 13 females in the control group, with an average gestational age of 37.66 ± 2.06 weeks, an average birth weight of 2.37 ± 0.68 kg, and an average age of admission of 3.66 ± 0.25 days. There was no significant difference between the two groups in the clinical data of gestational age and weight ($P > 0.05$), so general information is available. The newborn guardian understood the research and signed the informed consent form.

2.6. Treatment Methods. The patients' condition was confirmed by routine examination of abdominal standing and lying films, procalcitonin, C-reactive protein, electrolyte, blood routine examination, and defecation routine examination. Meanwhile, the patients' abdominal circumference and bowel sounds were monitored at any time during the treatment. Normal milk powder is not used for patients and breast milk is not used for children. According to the recommended feeding method in *the Chinese Clinical Application Guide of Neonatal Nutrition Support*, the infants in the treatment group were fed; that is, the infants with stable condition and strong breathing and strong sucking could be fed by mouth. If the gestational age or body weight is too small, those with poor sucking ability can be fed by nasogastric tube gradually to oral feeding. Premature infants with birth weight less than 1 kg and severe anoxia and asphyxia can delay the weaning time to 1-2 days after birth, and those with birth weight more than 1 kg and stable condition can start oral feeding within 1 day after birth. In the treatment group, newborns were fed for only two weeks of Nestlé's deep hydrolytic protein milk powder, and two weeks later, the children were observed to try to change into ordinary milk powder. During the transfer, 1/4 of the infant's common milk powder was mixed with deep hydrolytic protein milk powder, and the infant's stool and eating were observed to be normal, then gradually adjusted to 1/2 of the mixture, and then all of them were converted into common milk powder. In case of abnormal stool characteristics, it is necessary to change to the last milk powder. All day long, if the feeding intolerance occurred, the feeding volume was

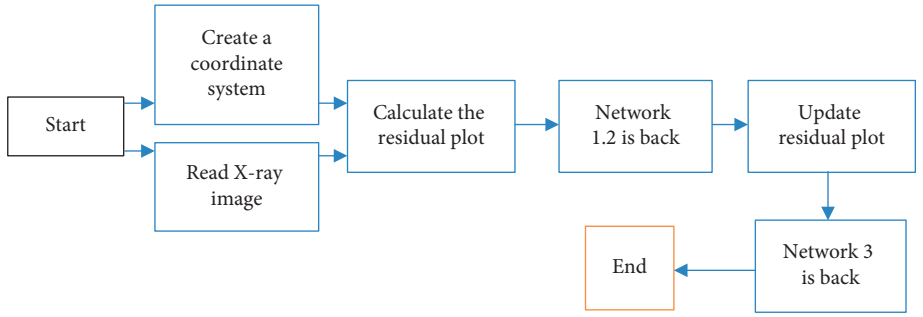

Figure 4: Flow chart of distribution regression.

Table 1: Internal structure of CNN network.

Layer	Input	Output
Batch normalization	4@258 × 258	4@258 × 258
2D convolution	4@258 × 258	64@258 × 258
RELU	64@258 × 258	64@258 × 258
Average pooling	64@258 × 258	64@258 × 258 4@258 × 258
Batch normalization	64@258 × 258	64@258 × 258
2D convolution	64@258 × 258	128@258 × 258
RELU	128@258 × 258	128@258 × 258
Average pooling	128@258 × 258	128@258 × 258

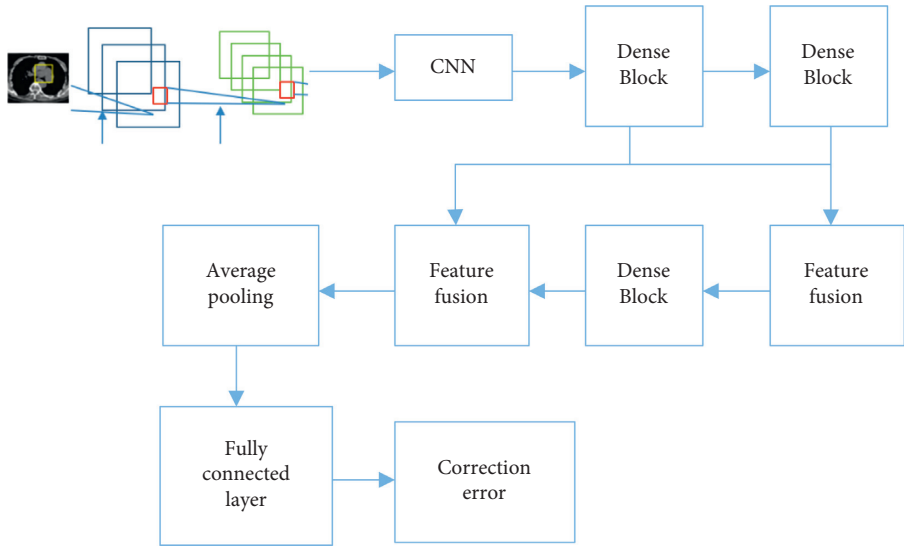

Figure 5: Network framework diagram.

adjusted according to the gastric retention. If the infant's stomach retention reached the 1/3 of the total feeding amount, the 1 time of the total feeding volume could be stopped. If the total amount of the day's feeding was less than half of that of the whole day, the next day's milk volume was the same as the previous day. If the vomiting occurs more than 3 times in 1 d during the feeding process and the gastric retention or vomit contains bile and coffee liquid, abdominal distension is aggravated, abdominal circumference increases more than 1.5 cm or with intestinal type, abdominal muscle tension and abdominal X-ray abnormalities occur, fecal occult blood positive or obvious bloody stool appear, bowel sounds weaken or disappear, and fasting and further diagnosis and treatment are needed. If the fasting time is less than 1 day, start feeding again, and the method is as above. In the control group, parenteral nutrition support was used, and 1 g/kg glucose liquid was given on the first day after birth and 1 g/kg amino acid fat emulsion was added on the second day according to *the Clinical Application Guide for Neonatal Nutrition Support in China*. The dosage of the two was gradually increased by 0.5–1 g to 3 g/kg amino acid fat emulsion and 10–12 mg/kg glucose per day under the stable

condition of the baby. At the same time, electrolytes, water-soluble fat-soluble vitamins, and microelements were dissolved in the nutrient solution and maintained by the micro infusion pump throughout the day. Before and after the infusion, the condition of the baby was observed regularly, the liver function of the baby was checked in time and the infection prevention work was done well. The treatment time of the two groups was two weeks, and the patients were followed up for two weeks after the treatment.

2.7. Observation Index. At the end of the treatment, the total effective rate, the time from recovery to birth weight, the time to complete gastrointestinal feeding, the time of fetal defecation, the speed of weight growth, and the incidence of feeding intolerance were compared between the two groups.

2.8. Evaluation Methods. When the child's stomach retention is greater than 50% of the feeding volume, accompanied by abdominal distension or vomiting, it is regarded as feeding intolerance. The effective rate of treatment in two groups can refer to literature [5]. The symptoms of infant abdominal distension basically disappeared, vomiting stopped, sucking improved, gastric retention decreased, and bowel sounds recovered as markedly effective. The symptoms of infant abdominal distension obviously improved, vomiting decreased, gastric remnant decreased, and sucking and bowel sounds improved which were regarded as effective. If the baby's abdominal distention is still the same, the residual amount of stomach, bowel sounds, and sucking force is not changed as before, and then it is considered as ineffective. The total effective rate + effective rate of the two groups.

The data training environment is as follows. The graphics card is Tesla P100 and the CPU is Intel E5-2680 server, and the deep learning framework PyTorch 0.4 is adopted to write training. In the training, the deep learning network is used for optimization. The training discussion Epoch is 32, and the size of the mini-Bach that is not sufficiently randomly selected in each round is 64. To compare the effect of the registration method, a comparison algorithm is used to accelerate the iterative dual X-ray image registration. The registration standard uses mTRE, and the registration parameter evaluates the error MSE.

$$\mathrm{mTRE} = \frac{1}{N}\sum_{T=1}^{N}\left\|T_{\mathrm{reg}}Qi - T_{gd}Qi\right\|. \tag{2}$$

The CT image contains a set Q of N points. When the change in the registration result is calculated, Treg and the target are exactly the mean distance error of the point corresponding to the change in T_{gd}. The physical size length of 2CT data is 1%, which is 2.83. As a criterion for successful registration, the MSE calculation is as follows:

$$\mathrm{MSE}(B) = \frac{1}{N}\sum_{T=1}^{N}\left\|B_i' - B_i\right\|. \tag{3}$$

B' is the vector of the registration parameters of B through the N unit translation. The registration parameters and the real parameters are used to calculate the translation and reversal MSE.

2.9. Statistical Methods. SPSS 17.0 was used, chi square test was used to compare the counting data, the results of measurement data were expressed in $(\overline{x} \pm S)$, t test was used to compare the measurement data, and the difference was statistically significant ($P < 0.05$).

3. Results

3.1. Sample Training. For the parameter regression training in one of the plane coordinate systems, the error of the translation parameter regression equation was 0.052 mm, which was a decrease of 83.6% relative to the iteration. The rotation parameter regression error was 0.068, which was a significant improvement (Figure 6).

3.2. Images. Figures 7(a) and 7(b) are X-ray images of two children. Figure 7(b) shows that there was an abnormality on the right side of the children. The abnormal bowel sounds were detected in children, and routine tests were performed on the children's C-reactive protein, electrolytes, and stool for the next step of analysis. Figure 8(a) shows the CNN algorithm image diagram, Figure 8(b) shows the Compute Unified Device Architecture (CUDA) algorithm image diagram, Figures 8(c) and 8(d) are the local feature extraction diagram, and the red box in the image showed the feature extraction part.

3.3. Result Comparisons. The running times and MSE values of the two algorithms were compared, and the results are shown in Figure 9. The CNN running time was 0.053 s, the CUDA running time was 12.409 s, and the CNN algorithm was significantly lower than the CUDA algorithm; the difference was statistically significant ($P < 0.05$). The error MSE of the CNN algorithm was 0.041 mm, and the error of CUDA was 0.301. That of CNN algorithm was obviously more accurate than the CUDA algorithm, and the difference was statistically significant ($P < 0.05$).

3.4. Comparison of the Effective Rate of Treatment between Two Groups of Children. After treatment, the total effective rate of the treatment group is 92.86%, and the effective rate of the treatment group is 9%. The total effective rate of the treatment group was significantly higher than that of the control group ($P < 0.05$), as shown in Table 2.

3.5. Comparison of Recovery Time to Birth Weight, Total Gastrointestinal Feeding Time, Defecation Time, and Weight Growth Rate between the Two Groups. Compared with the control group, the recovery time of total gastrointestinal feeding, the recovery time of birth weight, and the time of defecation in the treatment group were significantly shorter than that in the control group, and the growth rate of body weight was also faster than that in the control group ($P < 0.05$), as shown in Table 3.

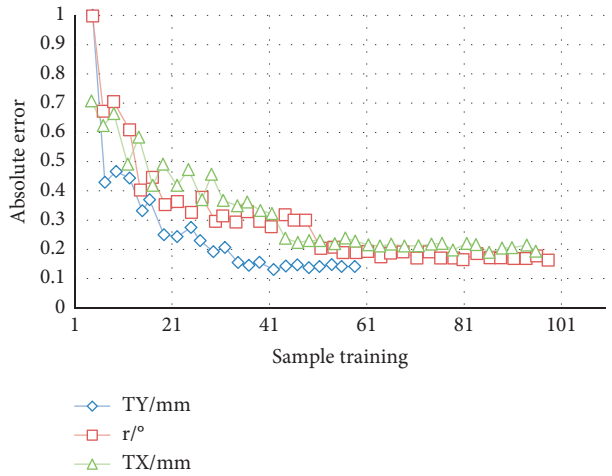

Figure 6: Parameter regression training error in the plane coordinate system.

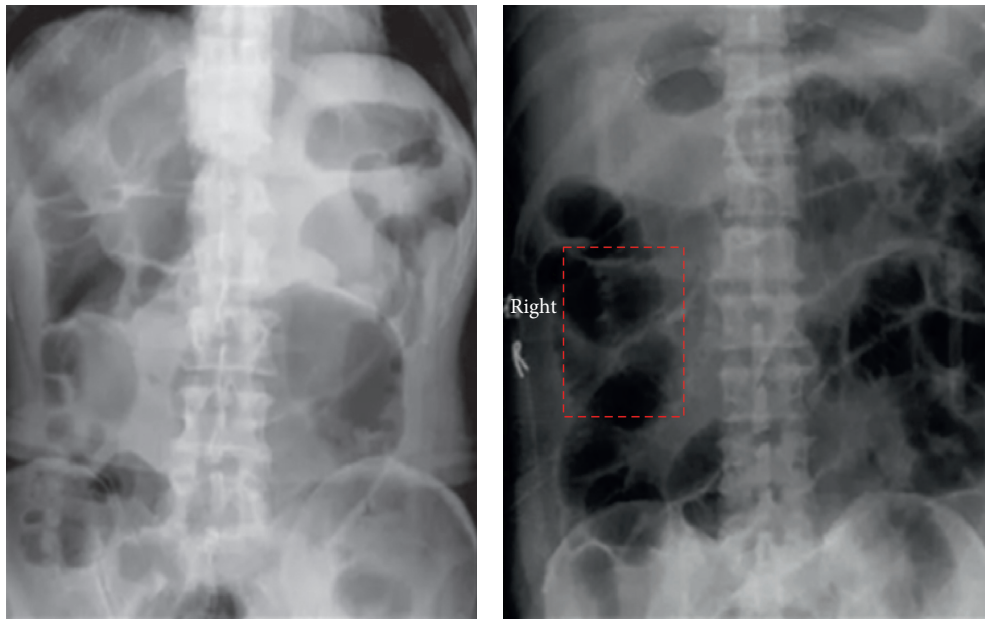

(a) (b)

Figure 7: Images: (a) child, male, 36 weeks old and (b) child, female, 38 weeks old.

3.6. Comparison of Feeding Intolerance in Two Groups. The incidence of feeding intolerance was 3.57% (1/28) in the treatment group and 36.36% (8/22) in the control group. The incidence of feeding intolerance in the treatment group was significantly lower than that in the control group ($X^2 = 4.26$, $P < 0.05$) (Figure 10).

4. Discussion

The development of digestive system of newborn is slow and the function is not perfect, so there are many cases of noninfectious abdominal distention. For example, due to the slow gastrointestinal peristalsis, dyspepsia often occurs, and the stool characteristics and times are abnormal. The newborns fed with milk powder are allergic to milk powder, feeding intolerance, crying, and swallowing a lot of gas, resulting in pneumoperitoneum and noninfectious abdominal distention [13, 14]. Neonatal abdominal distention is generally accompanied by other digestive system discomfort, such as constipation, diarrhea, stomachache, or sleep instability. Abdominal distention is a sign of intestinal dysfunction in children [15]. After abdominal distention, the newborn can only express discomfort through crying, but the crying aggravates the swallowing gas and leads to more serious inflation. Moreover, the newborn adopts abdominal breathing, with high respiratory frequency. The inflation can significantly affect the newborn's compensatory ability, reduce the gas exchange rate, and affect the growth and development of all aspects of the newborn [16, 17]. At the same time, the newborn with abdominal distention is prone to

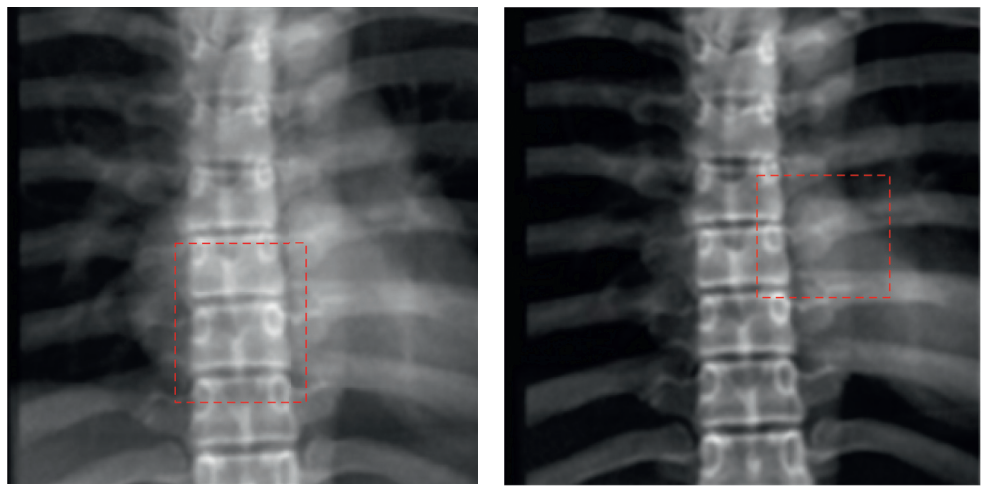

(a) (b)

Figure 8: Continued.

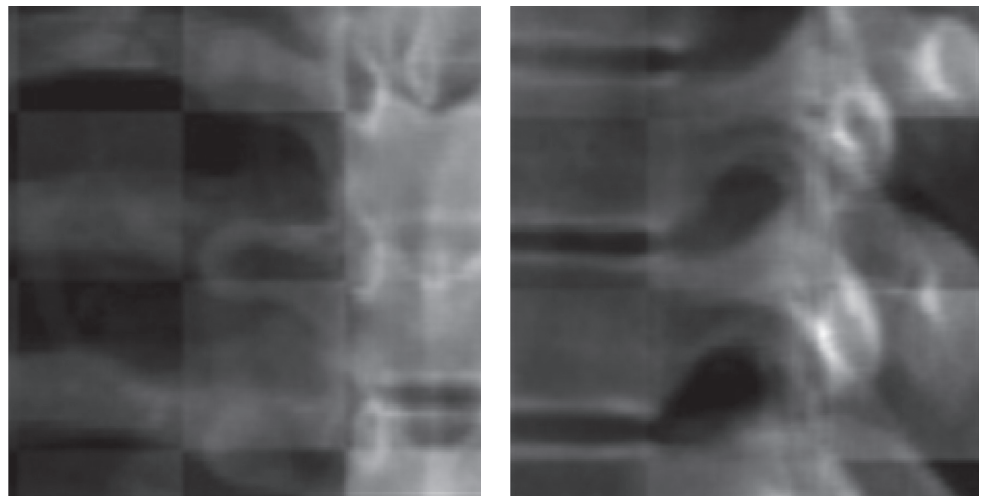

(c) (d)

Figure 8: Image comparison between CNN algorithm and CUDA algorithm.

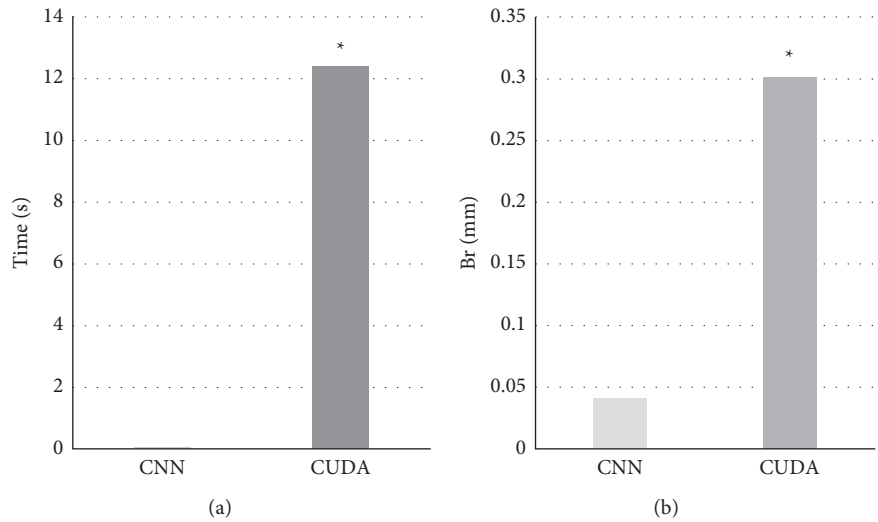

(a) (b)

Figure 9: Running time and MSE comparison between CNN algorithm and CUDA algorithm. Note. * indicates that the difference with CNN was statistically significant ($P < 0.05$).

Table 2: Comparison of the effective rate of treatment between two groups of children.

Name of group	Number of cases	Markedly effective	Effective	Ineffective	Total effective rate
Treatment group	28	17 (60.71)	9 (32.14)	3 (7.14)	92.86%
Control group	30	8 (26.67)	10 (33.33)	12 (40.00)	60.00%
X^2					6.84
P					<0.01

Table 3: Comparison of recovery time to birth weight, total gastrointestinal feeding time, defecation time, and weight growth rate between the two groups.

Name of group	Number of cases	Recovery time to birth weight (d)	Total gastrointestinal feeding time (d)	Defecation time (d)	Weight growth rate (g/d)
Treatment group	28	9.54 ± 1.45	13.23 ± 2.07	4.79 ± 0.65	17.51 ± 2.35
Control group	30	$11.72 \pm 1.68^*$	$18.52 \pm 2.64^*$	$6.07 \pm 1.52^*$	$13.11 \pm 3.42^*$
t		5.273	8.451	4.11	5.67
P		<0.001	<0.01	<0.01	<0.01

Note. * indicates that the difference was statistically significant compared with the treatment group ($P < 0.05$).

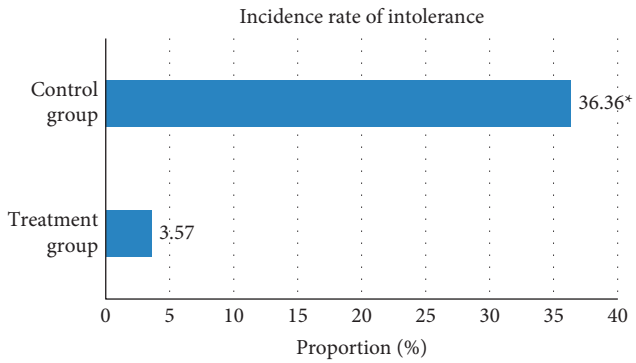

Figure 10: Incidence rate of neonatal intolerance in two groups. Note. * indicates that the difference was statistically significant compared with the treatment group ($P < 0.05$).

multiple symptoms, such as endless feces, vomiting, feeding intolerance, and even necrotizing enteritis, which is a serious threat to the health and life of the newborn. Therefore, it is necessary to pay attention to the situation of neonatal abdominal distention and identify the causes for timely treatment. Because noninfectious abdominal distention is often a complication, it is often caused by the incomplete gastrointestinal function of the newborn. During the treatment, patients can be helped by speeding up the peristalsis in the intestine, feeding outside the intestine, and relieving the pressure. Abdominal massage and parenteral vein injection are common treatment methods.

The application of deep learning in imaging can complete a variety of imaging techniques, with high image quality. The virtual endoscopy not only is realistic but also improves the detection rate of smaller lesions and mucosal lesions, which effectively improves the image. CNN is often used to learn original images in medicine and is widely used in image segmentation, image classification, and target image positioning [18]. Some scholars proposed that combining pixel information of different scales can extract the best size information [19]. Some researchers believed that reducing the size of the convolution kernel can improve the running speed of the neural network [20]. X-DRR image is a highly nonlinear function of spatial transformation parameters. In the traditional iterative process, it is very likely to fall into the local optimal value, which will cause registration errors. For a trained neural network, only one one-way calculation is required for the residual image during registration. There is no need to iteratively generate digitally reconstructed radiographic images and calculate image similarity, which avoids the most time-consuming part of traditional iterative optimization algorithms and has very fast registration capabilities. Zikic et al. [21] used the point set projection on the minimized 3D data to perform distance registration with the points on the 2D image. Jin et al. [22] used surgically implanted radiopaque artificial markers as features to increase the extraction of image features. The X-ray shooting process simulated in the computer made the ray tracing method project the CT DRR image. The CT space transformation parameters were optimized so that the similarity measurement function of the radiographic image reached the optimal value.

To a certain extent, massage can accelerate the gastrointestinal peristalsis, help the baby defecate and exhaust, and relieve the pressure of abdominal distention. But this is only for slight abdominal distention, which can be used as an auxiliary means of treatment. Parenteral feeding is a common means to provide nutritional support for newborns. It can provide the nutrition needed by newborns and ensure the survival of children. However, its disadvantages are also obvious. Parenteral nutrition can only be temporary. Newborns need to achieve parenteral nutrition finally. Besides the pain caused by puncture, it will also be accompanied by the risk of infection through venipuncture. At the same time, parenteral nutrition support also brings heavy economic burden to parents of children, which is unfavorable to the promotion of neonatal abdominal distention treatment [23].

The effects of deep hydrolytic protein milk powder and parenteral nutrition on noninfectious abdominal distention

of neonates have been compared. The results showed that the total effective rate of abdominal distention treatment of infants fed with deep hydrolytic protein milk powder two weeks later was significantly higher than that of infants fed with parenteral nutrition, suggesting that deep hydrolytic protein milk powder can effectively alleviate the symptoms of abdominal distention. The time of recovery to birth weight, total gastrointestinal feeding time, and fetal excretion time of children fed with deep hydrolyzed protein milk powder were significantly shorter than those fed with parenteral nutrition support, the growth rate of children's weight was also faster, and the incidence of feeding intolerance was significantly lower [24, 25]. It suggested that children's absorption of deep hydrolyzed protein milk powder was better and acceptance was higher, and children's stomach was more adaptable to DHP degree hydrolyzed protein milk powder. It may be due to the low activity of enterokinase and the weak digestion of protein in newborn, although parenteral nutrition support can provide the nutrients needed by newborn, due to the unstable formula of nutrient solution and the problem of the solubility of nutrients, its molecules are larger and the absorption effect of newborn is not good. Due to the special production process, the molecular weight of more than 95% of the deep hydrolyzed protein milk powder is less than 3000 daltons by enzymatic hydrolysis, heating, ultrafiltration, and other processing methods, which is very suitable for the delicate gastrointestinal absorption of newborns. At the same time, it has a stable formula, which can effectively reduce the antigenicity of protein components and greatly provide nutrients for newborns, and its short peptides and amino acids are more easily digested and absorbed by infants. For the newborns with immature digestive tract and low digestive enzyme activity, the deep hydrolyzed protein milk powder can help them to empty their stomach as soon as possible, improve the secretion of gastrointestinal hormones, shorten the transit time of milk in the gastrointestinal tract, promote digestion, help the newborns to recover normal defecation and exhaust, reduce gastroesophageal reflux, and shorten the feeding time of the whole gastrointestinal tract [26]. At the same time, without the pain and discomfort of repeated parenteral nutrition puncture, the newborn is less frightened and more stable in mood. This method is conducive to the recovery of birth weight as soon as possible and speeds up their daily growth and development. Meanwhile, the acceptance of parents will be higher.

In conclusion, the effect of deep hydrolyzed protein milk powder in the treatment of noninfective abdominal distention is significant, the recovery of children is fast, and the incidence of feeding intolerance is low, safe, and reliable.

5. Conclusion

In this study, a 2D-3D registration algorithm for dual X-ray images based on CNN was proposed. The orthogonal decomposition of spatial rigid body motion was transformed into two simple arrangements through convolution network processing. After the data training, the network completed the accurate dual-ray registration in 0.04 s. CNN network improved the accuracy of 2D-3D registration. Deep hydrolyzed protein milk powder had remarkable therapeutic effect on neonates. In addition, there was no infective abdominal distension, but fast recovery and low incidence of feeding intolerance, which suggested that it was safe and reliable. 2D-3D registration algorithm based on deep learning network is a potential method. A new registration algorithm based on dual X-rays was proposed. The limitation of this study was that the convergence range and rotation range of 2D-3D registration algorithm were difficult to set, and the system error could not be avoided, which needed to be improved later. In general, it is difficult to obtain massive medical images with labels, and it is necessary to configure the results manually. Nevertheless, it also provides a new direction for the development of semi-supervised and unsupervised deep learning algorithms, minimizing the need for data volume.

Data Availability

The data used to support the findings of this study are available from the corresponding author upon request.

Conflicts of Interest

The authors declare no conflicts of interest.

References

[1] Q. Cui, "Effect of Deep Hydrolyzed Protein Formula on Early Feeding of Premature infants," *Clinical Medicine Research and Practice*, vol. 2, no. 18, 2017.

[2] A. Chen, J. Du, and L. Z. Du, "Clinical characteristics of abdominal distention in early newborns," *Zhong Guo Dang Dai Er Ke Za Zhi*, vol. 15, no. 12, pp. 1074–1078, 2013.

[3] I. A. Schierz, M. Giuffrè, E. Piro et al., "Predictive factors of abdominal compartment syndrome in neonatal age," *American Journal of Perinatology*, vol. 31, no. 1, pp. 49–54, 2014.

[4] J. D. Zhang, W. M. Ou, M. H. Deng, and J. F. Zhang, "Effect of deep hydrolyzed protein formula milk powder on children with allergic asthma induced by milk powder," *Bethume Journal of Medicine*, vol. 14, no. 5, pp. 564–566, 2016.

[5] Y. Xiao, J. Wu, Z. Lin, and X. Zhao, "A deep learning-based multi-model ensemble method for cancer prediction," *Computer Methods and Programs in Biomedicine*, vol. 153, pp. 1–9, 2018.

[6] S. L. Al-Khafaji, J. Zhou, A. Zia, and A. W.-C. Liew, "Spectral-spatial scale invariant feature transform for hyperspectral images," *IEEE Transactions on Image Processing*, vol. 27, no. 2, pp. 837–850, 2018.

[7] M. Hu, Y. Zhong, S. Xie, H. Lv, and Z. Lv, "Fuzzy system based medical image processing for brain disease prediction," *Frontiers in Neuroscience*, vol. 15, Article ID 714318, 2021.

[8] Z. Wan, Y. Dong, Z. Yu, H. Lv, and Z. Lv, "Semi-supervised support vector machine for digital twins based brain image fusion," *Frontiers in Neuroscience*, vol. 15, Article ID 705323, 2021.

[9] L. Zou, S. Yu, T. Meng, Z. Zhang, X. Liang, and Y. Xie, "A technical review of convolutional neural network-based mammographic breast cancer diagnosis," *Comput Math Methods Med*, vol. 2019, Article ID 6509357, 16 pages, 2019.

[10] Y. Lei and Z. Yan, "An improved 2D-3D medical image registration algorithm based on modified mutual information and expanded powell method," in *Proceedings of the 2013 IEEE International conference on medical Imaging physics and engineering*, pp. 24–29, Shenyang, China, October 2013.

[11] S. Ghafurian, I. Hacihaliloglu, D. N. Metaxas, V. Tan, and K. Li, "A computationally efficient 3D/2D registration method based on image gradient direction probability density function," *Neurocomputing*, vol. 229, pp. 100–108, 2017.

[12] M. M. A. Monshi, J. Poon, and V. Chung, "Deep learning in generating radiology reports: a survey," *Artificial Intelligence in Medicine*, vol. 106, Article ID 101878, 2020.

[13] R. Listernick, "An 8-day-old boy with abdominal distention after oral feeding," *Pediatric Annals*, vol. 43, no. 10, pp. 383–385, 2014.

[14] J. E. Dalziel and W. Young, "Gastric emptying and gastrointestinal transit compared among native and hydrolyzed whey and casein milk proteins in an aged rat modelr," *Nutrients*, vol. 9, no. 12, 2017.

[15] N. Bansal and T. Truong, "Feasibility Study of Lecithin Nanovesicles as Spacers to Improve the Solubility of Milk Protein Concentrate Powder during storage," *Dairy Science & Technology*, vol. 96, pp. 861–872, 2017.

[16] G. S Meena, "Effect of change in pH of skim milk and ultrafiltered/diafiltered retentates on milk protein concentrate (MPC70) powder properties," *Journal of Food Science & Technology*, vol. 55, no. 9, pp. 3526–3537, 2018.

[17] S. Pathania, "Applications of hydrodynamic cavitation for instant rehydration of high protein milk powders," *Journal of Food Engineering*, vol. 225, pp. 18–25, 2018.

[18] Z. Lv, L. Qiao, Q. Wang, and F. Piccialli, "Advanced machine-learning methods for brain-computer interfacing," *IEEE/ACM Transactions on Computational Biology and Bioinformatics*, vol. 18, no. 5, pp. 1688–1698, 2021.

[19] H. J. Wisselink, G. J. Pelgrim, M. Rook et al., "Ultra-low-dose CT combined with noise reduction techniques for quantification of emphysema in COPD patients: an intra-individual comparison study with standard-dose CT," *European Journal of Radiology*, vol. 138, Article ID 109646, 2021.

[20] E. Oh, S. W. Seo, Y. C. Yoon, D. W. Kim, S. Kwon, and S. Yoon, "Prediction of pathologic femoral fractures in patients with lung cancer using machine learning algorithms: comparison of computed tomography-based radiological features with clinical features versus without clinical features," *Joures of Orthopaedic Surgery*, vol. 25, no. 2, p. 1022, 2017.

[21] D. Zikic, M. Groher, A. Khamene, and N. Navab, "Deformable Registration of 3D Vessel Structures to a single projection image," *Medical imaging 2008: image processing*, vol. 6914, Article ID 691412, 2008.

[22] J.-Y. Jin, S. Ryu, K. Faber et al., "2D/3D Image fusion for accurate target localization and evaluation of a mask based stereotactic system in fractionated stereotactic radiotherapy of cranial lesions," *Medical Physics*, vol. 33, no. 12, pp. 4557–4566, 2006.

[23] P. Zhang, "Study on screening potential allergenic proteins from infant milk powders based on human mast cell membrane chromatography and histamine release assays," *Journal of European Economy*, vol. 9, no. 1, 2019.

[24] Q. Line and Q. L. Bendtsen, "Human muscle protein synthesis rates after intake of hydrolyzed porcine-derived and cows' milk whey proteins-A randomized controlled trial," *Nutrients*, vol. 11, no. 5, 2019.

[25] J. Fitzpatrick and S. Wu, "The Effect of pH on the Wetting and Dissolution of Milk Protein Isolate powder," *Journal of Food Engineering*, vol. 240, pp. 114–119, 2019.

[26] J. Singh and S. Prakash, "Comparison of ultra high temperature(UHT) stability of high protein milk dispersions prepared from milk protein concentrate(MPC) and conventional low heat skimmed milk powder(SMP)," *Journal of Food Engineering*, vol. 246, pp. 86–94, 2019.